Table S1. Effects of MTS modification on receptors incorporating NR1wt and the indicated NR2 mutant

| NR2 mutant | Relative current (mean ± s.d.) | | |
|---|---|---|---|
| | post MTSEA | post MTSET | post MTS-PtrEA |
| **NR2B mutant** | | | |
| H127C | 1.13 ± 0.03 (n=5) | 1.29 ± 0.06 (n=5) | 1.58 ± 0.10 (n=8) |
| H127A | 0.93 ± 0.01 (n=7) | 0.84 ± 0.03 (n=5) | 0.74 ± 0.01 (n=5) |
| Y282C | 2.1 ± 0.1 (n=10) | 4.4 ± 0.6 (n=10) | 5.5 ± 1.0 (n=33) |
| Y282S | 0.91 ± 0.02 (n=4) | 0.92 ± 0.03 (n=4) | 0.92 ± 0.02 (n=4) |
| **NR2A mutant** | | | |
| H128C | 0.74 ± 0.01 (n=6) | 0.83 ± 0.02 (n=8) | 0.91 ± 0.10 (n=10) |
| H128S | 0.80 ± 0.01 (n=4) | 0.76 ± 0.01 (n=4) | 0.84 ± 0.07 (n=6) |
| Y281C | 1.02 ± 0.02 (n=12) | 1.09 ± 0.04 (n=6) | 0.95 ± 0.03 (n=6) |
| Y281A | 0.60 ± 0.06 (n=12) | 0.58 ± 0.04 (n=6) | 0.58 ± 0.03 (n=5) |

Table S2. pH sensitivity of receptors incorporating NR1wt and the indicated NR2 construct

| NR2 construct | $pH_{IC50}$ |
|---|---|
| NR2Awt | 6.93 ± 0.02 (n=9) |
| NR2Bwt | 7.50 ± 0.03 (n=5) |
| NR2A-ΔNTD | 7.11 ± 0.09 (n=9) |
| NR2B-ΔNTD | 7.14 ± 0.03 (n=6) |
| NR2A-(2B NTD+L) | 7.26 ± 0.03 (n=4) |
| NR2B-(2A NTD+L) | 7.02 ± 0.02 (n=4) |
| NR2Dwt | 7.52 ± 0.03 (n=10) |
| NR2D-(2A NTD+L) | 7.13 ± 0.01 (n=5) |

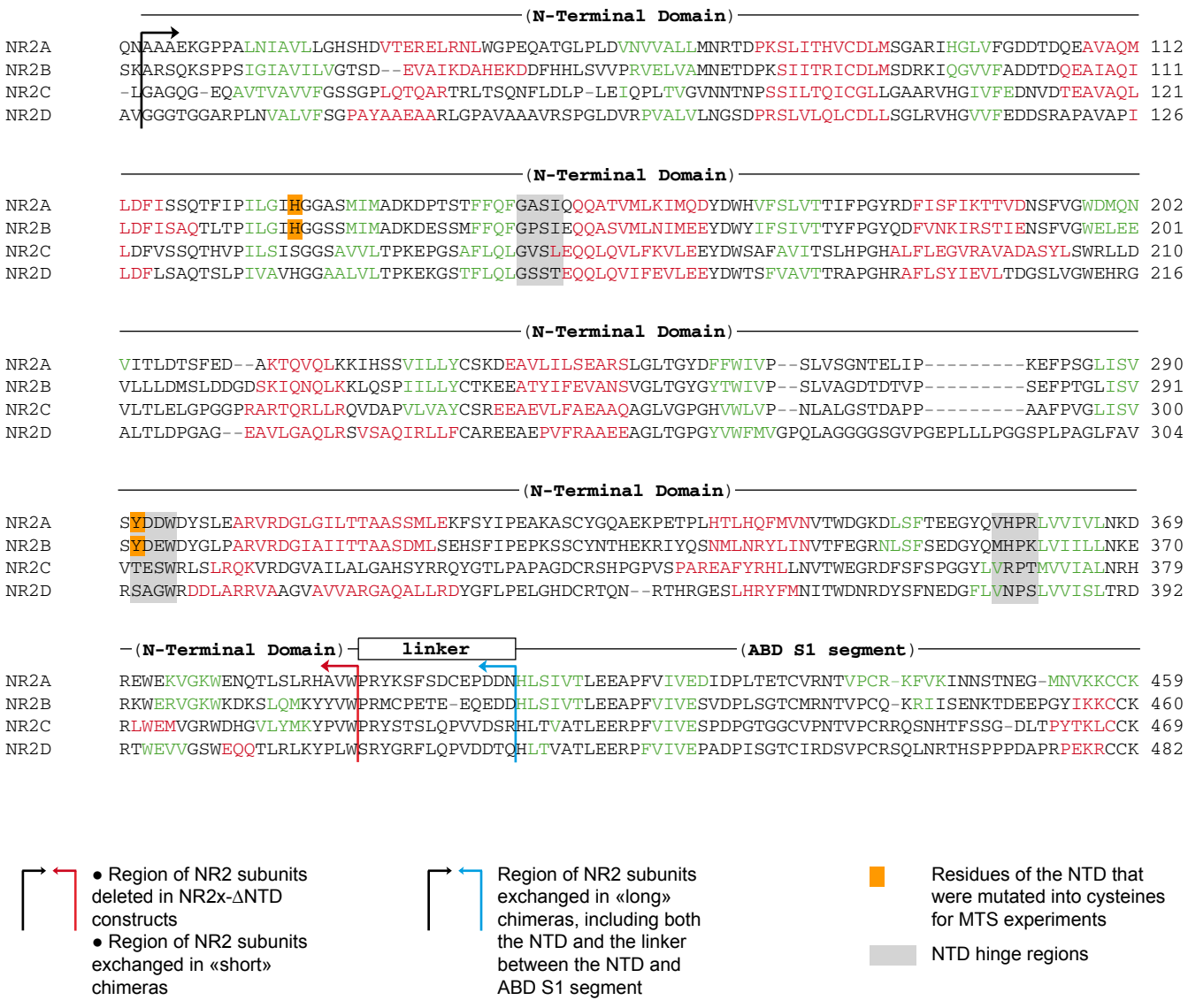


**Figure S1. Sequence alignment of the NTD+linker region of NR2A-D subunits**

The indicated α-helices (red) and β-strands (green) of NR2 subunits were predicted as described in ref[25].

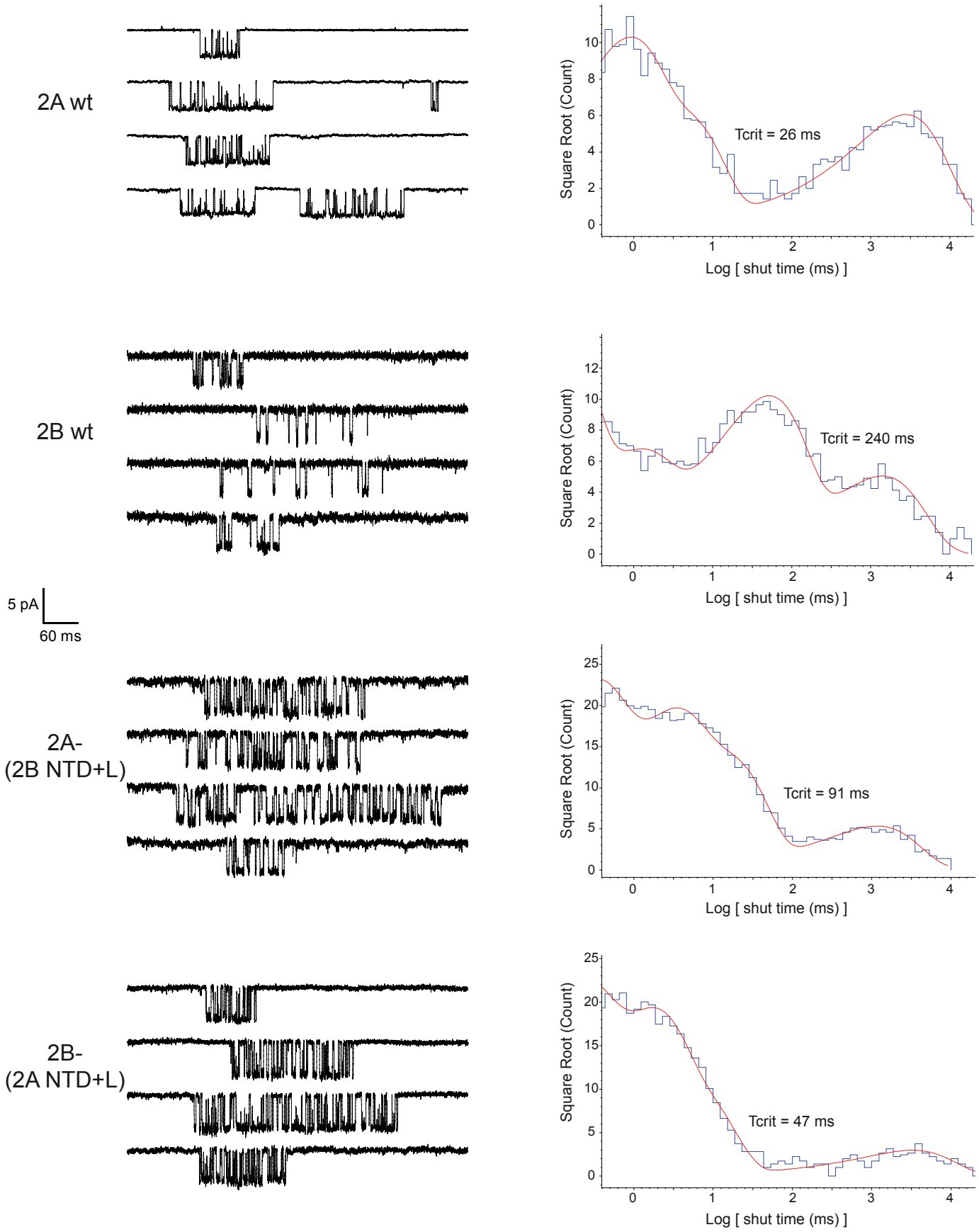


**Figure S2. Effect of NR2A/B NTD+L chimeras on single-channel activity**

Representative bursts of openings (left) and shut-time distribution histograms (right) from outside-out patches expressing either NR1wt/NR2Awt, NR1wt/NR2Bwt, NR1wt/NR2A-(2B NTD+L) and NR1wt/NR2B-(2A NTD+L). The value of Tcrit used to define bursts is indicated for each histogram.

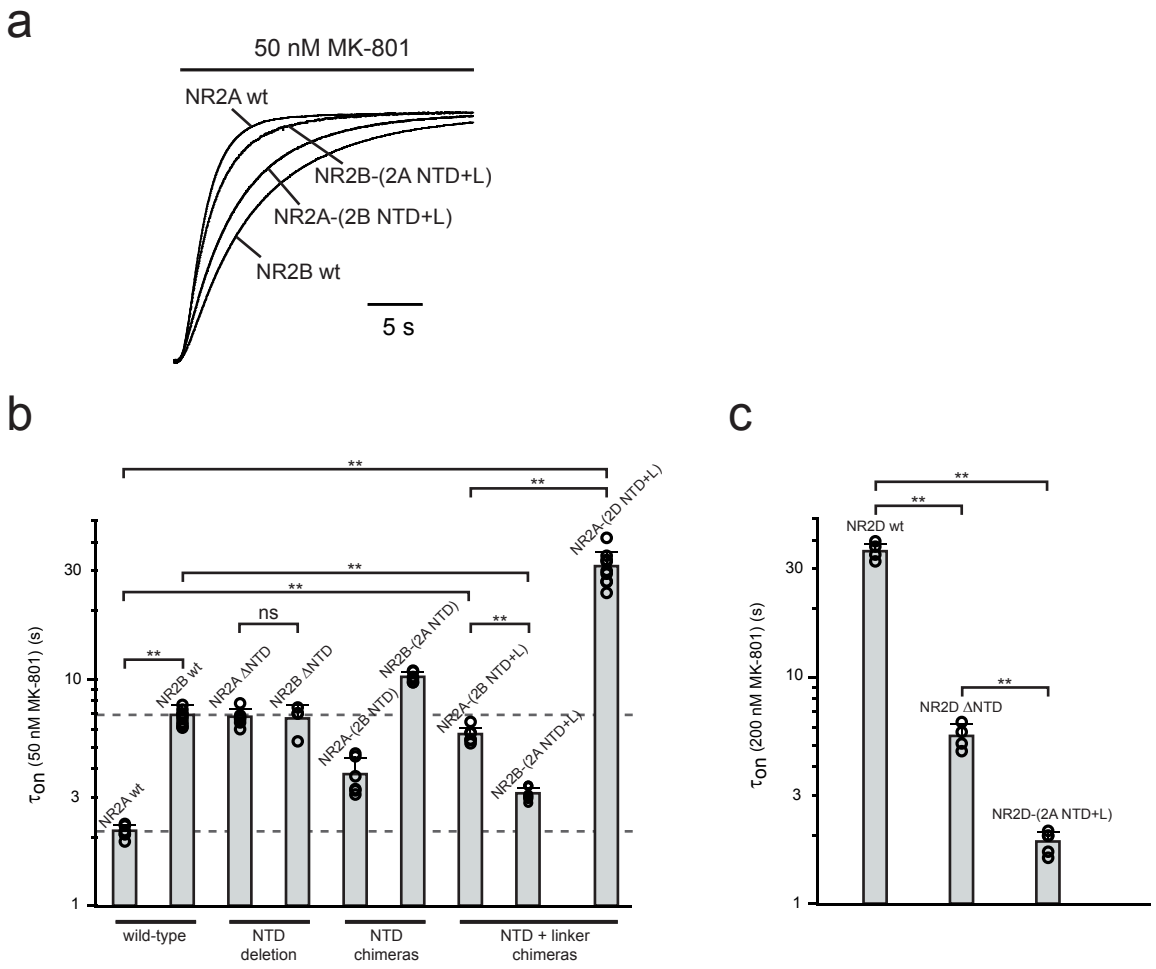


**Figure S3. Kinetics of MK-801 inhibition reveal that NMDAR Po heterogeneity is controlled by the NR2 NTD+linker region**

**a** Kinetics of inhibition by 50 nM MK-801 of receptors incorporating NR1wt together with NR2Awt ($\tau_{on}$ = 2.0 s), NR2Bwt (6.9 s), NR2A-(2B NTD+L) (5.1 s) or NR2B-(2A NTD+L) (2.8 s). **b** Bar graph showing the time constant of inhibition by 50 nM MK-801 of receptors incorporating NR1wt together with NR2Awt ($\tau_{on}$ = 2.1 +/- 0.1 s [n=6]), NR2Bwt (6.9 +/- 0.7 s [n=10]), NR2A-ΔNTD (6.8 +/- 0.6 s [n=6]), NR2B-ΔNTD (6.7 +/- 1.0 s [n=4]), NR2A-(2B NTD) (3.8 +/- 0.3 s [n=6]), NR2B-(2A NTD) (10.2 +/- 0.5 s [n=6]), NR2A-(2B NTD+L) (5.7 +/- 0.4 s [n=6]), NR2B-(2A NTD+L) (3.1 +/- 0.2 [n=9]) or NR2A-(2D NTD+L) (31.4 +/- 4 .9 s [n=10]) (**p<0.001). **c** Bar graph showing the time constant of inhibition by 200 nM MK-801 of receptors incorporating NR1wt together with NR2Dwt (36 +/- 3 s [n=5]), NR2D-ΔNTD (5.5 +/- 0.7 s [n=6]) or NR2D-(2A NTD+L) (1.9 +/- 0.2 [n=5]). Error bar represent s.d.

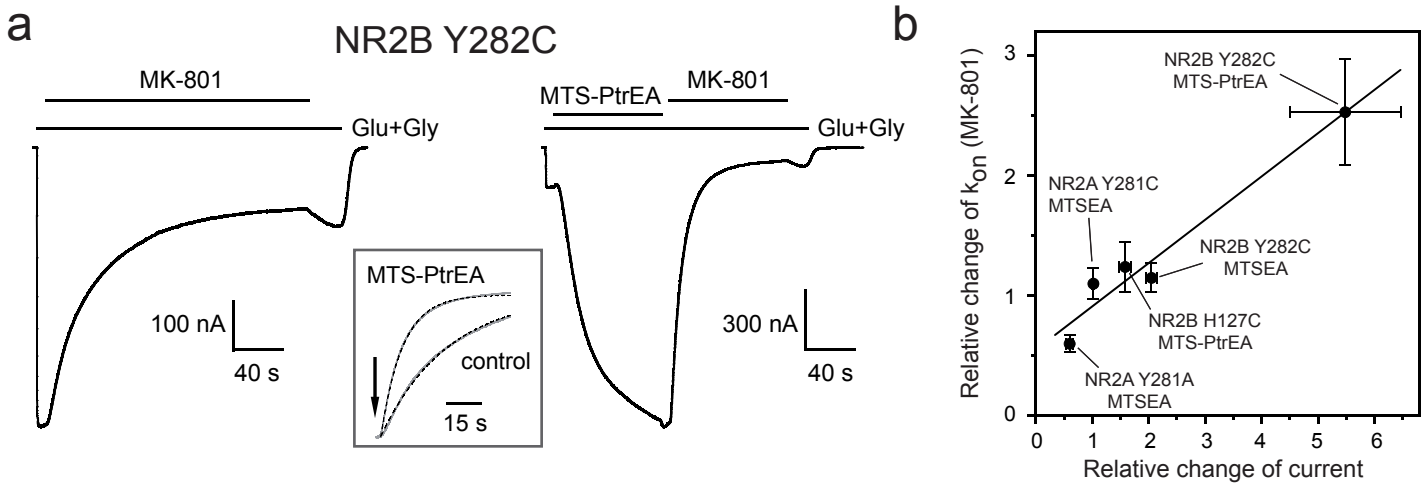


**Figure S4. Locking open the NR2-NTD increases the onset of MK-801 inhibition**

**a** Recordings showing the inhibition by 50 nM MK-801 of NR1wt/NR2B-Y282C receptors in the presence of 100 µM glutamate and 100 µM glycine before (left panel) and after (right panel) modification by 0.2 mM MTS-PtrEA. *Inset:* onsets of MK-801 inhibition shown in panel *a* were fitted with a single exponential ($\tau_{on}$ = 9.7 s before and 30 s after MTS-PtrEA). **b** The MTS-induced relative change of the MK-801 on-rate is plotted versus the MTS-induced relative change of the current for NR1wt/NR2A-Y281A (0.60 +/- 0.07 [n=4] vs 0.60 +/- 0.02 [n=12] with MTSEA, respectively), NR1wt/NR2A-Y281C (1.10 +/- 0.13 [n=4] vs 1.02 +/- 0.06 [n=12] with MTSEA, respectively), NR1wt/NR2B-H127C (1.24 +/- 0.21 [n=4] vs 1.58 +/- 0.10 [n=8] with MTS-PtrEA, respectively) and NR1wt/NR2B-Y282C (1.15 +/- 0.12 [n=4] vs 2.1 +/- 0.1 [n=9] with MTSEA, respectively; and 2.5 +/- 0.4 [n=4] vs 5.5 +/- 1.0 [n=33] with MTS-PtrEA, respectively). The line represents a linear regression fit of the data points. The R value of the fit is 0.98. Error bars represent s.d.

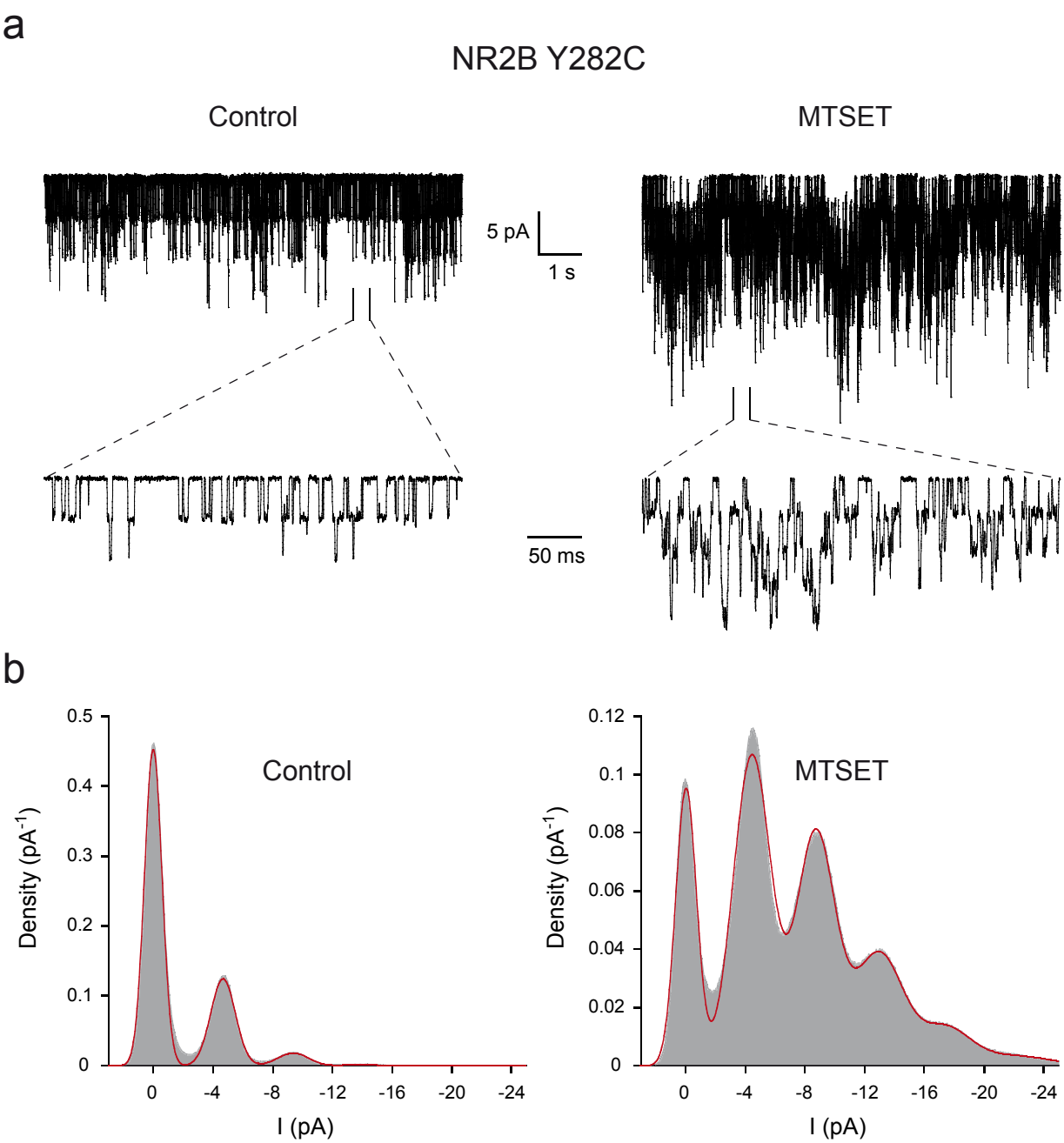


**Figure S5. Locking open the NR2-NTD increases single-channel activity**

**a** Single-channel recordings of an outside-out patch from a HEK cell expressing NR1wt/NR2B-Y282C receptors, in the presence of 100 µM glutamate and 100 µM glycine, before (left panel) and during (right panel) application of 0.2 mM MTSET. Bottom traces display time-expanded views. **b** All-points amplitude histograms from the patch recorded in *a*. Data (gray filling) were fitted with multiple gaussian components (red lines), amplitude of which enabled the calculation of N*Po before and during MTSET application. Similar results were obtained with 3 patches, yielding a mean potentiation of Po by MTSET of 3.4 +/- 0.5 (s.e.m.). Data were filtered at 5kHz for analysis and at 1 kHz for display.

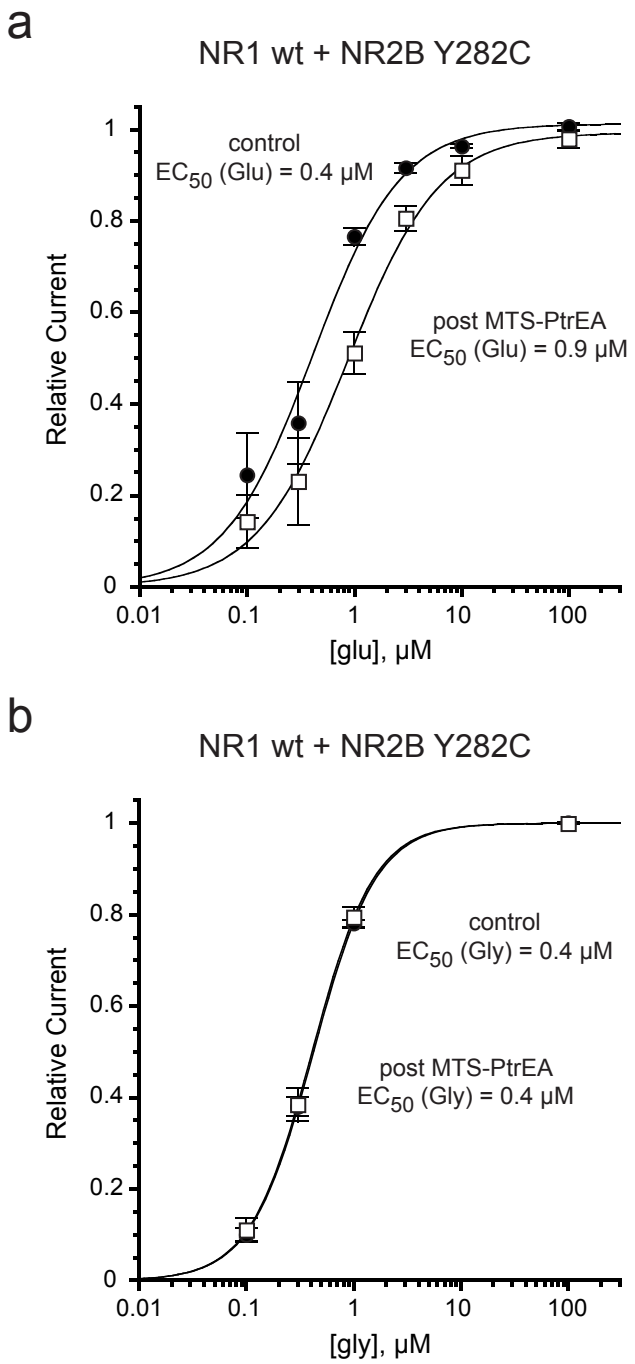


**Figure S6. Effect of MTS modification of NR1wt/NR2B-Y282C receptors on glutamate and glycine sensitivities**

**a** Glutamate dose-response curves of NR1wt/NR2B-Y282C receptors in the presence of 100 µM glycine before ($EC_{50}$ = 0.38 µM, $n_H$ = 1.2 [n = 9]; black-filled circles) and after ($EC_{50}$ = 0.9 µM, $n_H$ = 1.0 [n = 9]; open squares) modification by 0.2 mM MTS-PtrEA. **b** Glycine dose-response curves of NR1wt/NR2B-Y282C receptors in the presence of 100 µM glutamate before ($EC_{50}$ = 0.4 µM, $n_H$ = 1.5 [n = 4]; black-filled circles) and after ($EC_{50}$ = 0.4 µM, $n_H$ = 1.5 [n = 9]; open squares) modification by 0.2 mM MTS-PtrEA. Error bars represent s.d.

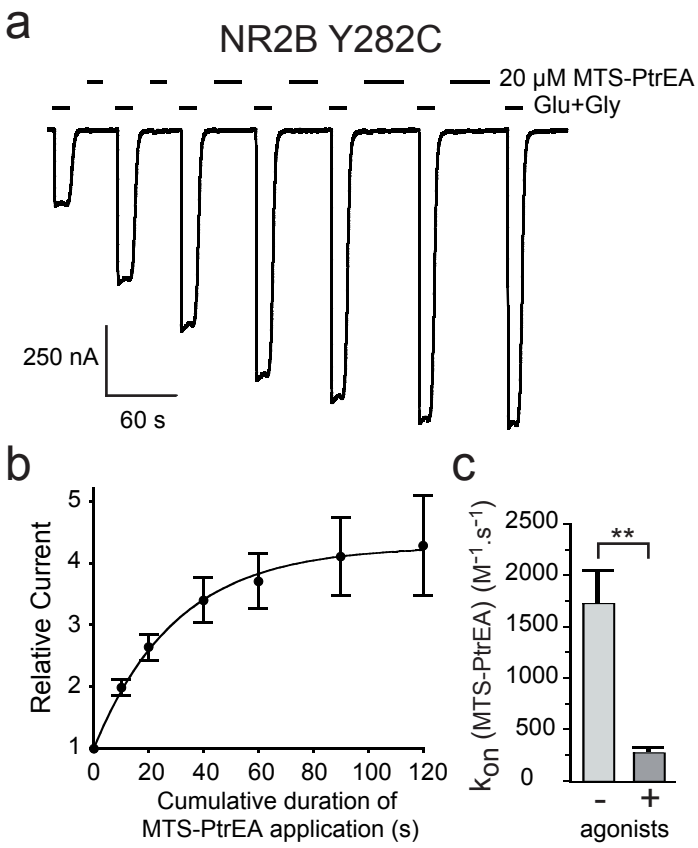


**Figure S7. MTS-PtrEA modification rate of NR1wt/NR2B-Y282C receptors is faster in the absence of agonists than in their presence**

**a** Recordings showing the modification of NR1wt/NR2B-Y282C receptors by 20 µM MTS-PtrEA in the absence of glutamate and glycine. **b** The onsets of MTS-PtrEA modification were fitted with a single exponential ($\tau_{on}$ = 30 +/- 6 s, [n=5]). **c** Mean reaction rate of MTS-PtrEA modification at NR1wt/NR2B-Y282C in the absence or in the presence of 100 µM glutamate and 100 µM glycine (1700 +/- 300 $M^{-1}.s^{-1}$ [n=5] and 280 +/- 50 $M^{-1}.s^{-1}$ [n=17], respectively) (**p<0.001, Student's t-test). Error bars represent s.d.

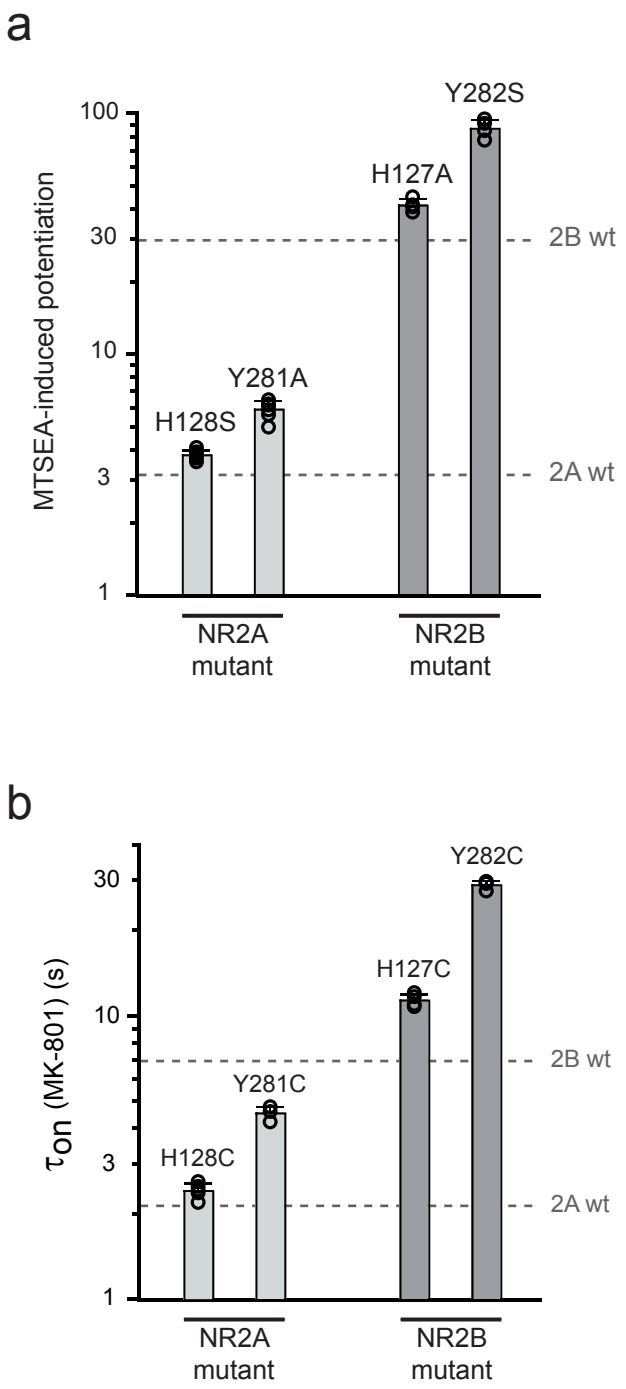


**Figure S8. Effect of NR2-NTD mutations on receptor activity**

**a** Bar graph showing the MTSEA-induced potentiations of receptors incorporating NR1-A652C together with NR2A-H128S (3.8 +/- 0.2, [n=7]), NR2A-Y281A (6.0 +/- 0.5, [n=7]), NR2B-H127A (42 +/- 2, [n=5]) or NR2B-Y282S (87 +/- 7, [n=3]). **b** Bar graph showing the onset of inhibition by 50 nM MK-801 of receptors incorporating NR1wt together with NR2A-H128C (2.4 +/- 0.2 s, [n=5]), NR2A-Y281C (4.6 +/- 0.2 s, [n=4]), NR2B-H127C (11.4 +/- 0.5 s, [n=4]) or NR2B-Y282C (29.1 +/- 0.9 s, [n=4]). Error bars represent s.d.

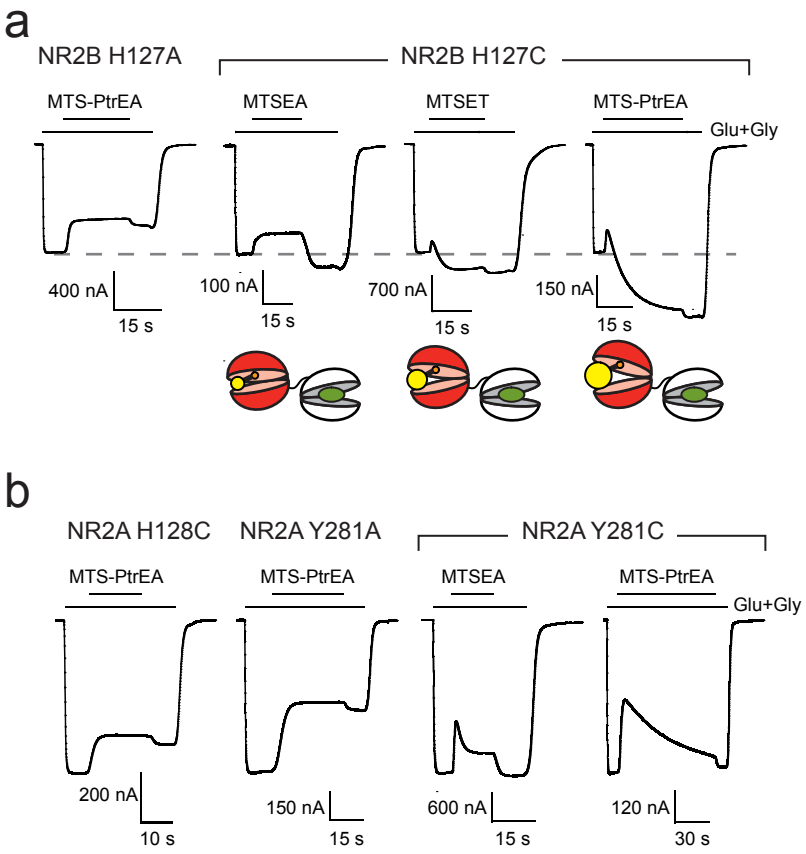


**Figure S9. Effect of MTS modification at NR2B-H127, NR2A-Y281 and NR2A-H128 mutated receptors**

**a** Recordings from NR1wt/NR2B-H127C and NR1wt/NR2B-H127A receptors during treatment by 0.2 mM of the indicated MTS compounds. **b** Recordings from NR1wt/NR2A-H128C, NR1wt/NR2A-Y281A and NR1wt/NR2A-Y281C receptors during treatment by 0.2 mM of the indicated MTS compound. Note that the MTS-potentiating effects are specific to the cysteine mutation introduced, since no potentiation were observed with the non-reactive serine or alanine control mutants, but rather an inhibition (likely due to the modification of an endogenous cysteine).